



Publication Year	2019
Acceptance in OA	2020-12-01T12:56:38Z
Title	New blazar candidates from the 9Y-MST catalogue detected at energies higher than 10 GeV
Authors	CAMPANA, RICCARDO, Massaro, E.
Publisher's version (DOI)	10.1007/s10509-019-3604-2
Handle	http://hdl.handle.net/20.500.12386/28598
Journal	ASTROPHYSICS AND SPACE SCIENCE
Volume	364

New blazar candidates from the 9Y-MST catalogue detected at energies higher than 10 GeV

R. Campana • E. Massaro

Abstract We present a list of 24 new blazar candidates selected in a search for possible counterparts of spatial clusters of γ -ray photons in the recent 9Y-MST catalogue, at energies higher than 10 GeV and at Galactic latitudes higher than 20° . 13 of these clusters are also included in the preliminary release of the 4FGL catalogue of γ -ray sources. The search for possible counterparts is based on the possible associations of the clusters with radio sources within a circle having a radius of $6'$. We then investigated the possible optical or mid-IR associations of these sources, checking if they show some properties typical of new blazar candidates.

Keywords γ -rays: observations – γ -rays: source detection

1 Introduction

The use of spatial clustering algorithms in the γ -ray sky allows to extract photon concentrations out of the diffuse background, which can be then associated with high energy cosmic sources. The multiwavelength analysis of the fields surrounding these photon clusters is useful to identify new sources that were missed in other surveys based on different selection criteria.

In a previous paper, we used the Minimum Spanning Tree (hereafter MST, Campana et al. 2008, 2013) method to produce a new catalogue of 1342 photon clusters, at Galactic latitudes $|b| > 20^\circ$ in the *Fermi*-Large

Area Telescope (LAT) dataset above 10 GeV and covering a 9 years time interval from the beginning of the mission (9Y-MST, Campana et al. 2018). The large majority of them correspond to sources already detected in previous searches, and generally were found to be closely associated with known BL Lac objects, Flat Spectrum Radio Quasars (FSRQ) and other Active Galactic Nuclei (AGN).

The 9Y-MST includes also 249 clusters without any correspondence with previously known high energy sources. As discussed in Campana et al. (2018) it is possible that a fraction of these unassociated photon clusters may be *spurious*, i.e. random fluctuations in the photon density, not related to any physical counterpart. However, many of these clusters were found having characteristic parameters quite close to those of the associated ones and therefore they may be actually related to cosmic sources not yet studied and classified. We searched for possible counterparts and obtained a sample of 24 spatial clusters of photons whose centroids have an angular separation from radio sources comparable to those found for clusters already associated with optical/IR objects exhibiting properties typical of blazars. In a series of papers (Bernieri et al. 2013; Campana et al. 2015, 2016a,b,c, 2017) we described the results of similar searches of possible new blazar counterparts of γ -ray clusters found by means of MST, which were, with a very few exceptions, confirmed by subsequent analyses.

In February 2019 the Fermi-LAT collaboration released a preliminary version of the 4FGL catalogue (The Fermi-LAT collaboration 2019), including 5098 γ -ray sources and reporting confirmed and candidate counterparts. In our selected sample of photon clusters, there are 13 out of 24 that correspond to 4FGL sources. Although they can be considered as *bona fide* γ -ray sources, we maintained them in the sample to al-

R. Campana

INAF/OAS-Bologna, via Gobetti 93, I-40129, Bologna, Italy.
riccardo.campana@inaf.it

E. Massaro

INAF/IAPS, via del Fosso del Cavaliere 100, I-00133, Roma, Italy

In Unam Sapientiam, Roma, Italy

low for a comparison of their observational properties with respect to other candidate sources.

The outline of this paper is as follows. In Section 2 and 3 we describe the criteria adopted for selecting the counterparts and present the resulting sample of new blazar candidates, in Section 4 the main properties of individual sources are given and in Section 5 the results are summarized and discussed.

2 Cluster parameters and counterpart selection criteria

For the preparation of the 9Y-MST catalogue we considered LAT data (Pass 8R2) above 10 GeV, covering the whole sky in the 9 years time range from the start of mission (2008 August 04) up to 2017 August 04, were downloaded from the FSSC archive¹. Standard cuts on the zenith angle, data quality and good time intervals were applied.

MST application and cluster selection criteria are described in the 9Y-MST paper (Campana et al. 2018), and therefore we describe here only the cluster parameters useful for source association and the search of possible counterparts. MST starts from considering the photon arrival directions in a given field as points (*nodes*) in a 2-D reference frame, and constructs a particular graph, the *minimum spanning tree*, connecting them with weighted *edges*. The edge weight is the angular distance between a pair of photon. Then, all the edges with a length below a threshold Λ_{cut} (expressed as a fraction of Λ_m , i.e. the average of all the edge lengths in the whole graph) are removed, as well as the remaining sub-trees with a number of nodes below a threshold N_{cut} . We refer to Campana et al. (2008, 2013) for details.

The main parameters of a cluster are its *photon number* n and the *clustering factor* g . The latter is defined as the ratio between the mean photon distance in the whole field Λ_m to the mean distance in the cluster itself ($\Lambda_{m,k}$, i.e. the average of all the edge lengths in the specific k -th sub-tree). This is a measure of the “clumpiness” of the cluster in consideration. The derived parameter M , the so called *magnitude* (Campana et al. 2013), is defined as the product $M = ng$ and was found to be related to the statistical significance of clusters.

Another parameter is the *cluster centroid* whose coordinates are computed as a weighted mean of the coordinates of the photons in the cluster. According to Campana et al. (2013), applying as a weight the inverse

of the square of the distance to the closest photon, it results a better agreement with the positions given by maximum likelihood (ML, Mattox et al. 1996) analysis. However, in the case of clusters with a low number of photons the weighted centroid may be biased if in the cluster there is a pair of photons much closer than the others: the centroid will be then located very close to this pair and the use of the unweighted mean can be more reliable.

Two other useful parameters are the *maximum radius* R_{max} , defined as the angular distance between the centroid and the farthest photon, that gives information on the overall extension of the cluster, and the *mean radius* R_m , the radius of the circle centred at the centroid and containing 50% of photons in the cluster, that for a point-like source should be smaller than or comparable to the 68% containment radius of instrumental Point Spread Function (PSF, see Ackermann et al. 2013).

The search for possible counterparts of unassociated clusters was aimed to select a sample of objects exhibiting one or more interesting properties to be considered blazar candidates. On the basis of a positional matching between the 9Y-MST and the 3FHL (Ajello et al. 2017) catalogues, Campana et al. (2018) found that more than 99% of associations are within an angular separation $\delta < 6'$, computed using the cluster centroid and the 3FHL coordinates, and this figure was used for searching other associations with lists of known blazars or candidates. In the present work we adopted the same criterion and defined a search region having a radius of $6'$ within to select new candidates.

Our first step was to extract from the NVSS² (1.4 GHz) and SUMSS21³ (0.835 GHz) catalogues — which together cover the entire sky — all the radio sources found in the searching region, to investigate if at least one of them would exhibit typical blazar features. For the association we used also the more severe positional criterion $\delta < R_{\text{max}}$. However, in the case of low g clusters this choice could be problematic because R_{max} may have large variations depending on the selection parameters. A more detailed analysis of the cluster structure was therefore performed to obtain a good association. We also extended the search for data to optical and X-ray bands in order to verify whether radio counterparts might be associated with sources exhibiting some blazar properties. We thus obtained a sample of 24 γ -ray clusters that is listed in Table 1 together with the coordinates and names of selected candidate counterparts. In the next Section 4 the properties of these candidates are presented individually.

²<https://www.cv.nrao.edu/nvss/>

³<http://www.astrop.physics.usyd.edu.au/sumsscat/>

¹<http://fermi.gsfc.nasa.gov/ssc/data/access/>

3 WISE colours

After the selection of radio candidates, we searched for possible optical and mid-IR (AllWISE catalogue, Cutri et al. 2013) counterparts having coordinates within their uncertainty radii, typically few arcseconds, and tested if their photometric data are compatible with a blazar nature. More specifically, a very useful test is to check if the mid-IR colours are located within the *WISE Gamma-ray Strip* according to the definition of Massaro and D’Abrusco (2016).

We obtained three-band infrared photometric data from the AllWISE catalogue: for 18 out of 24 cluster candidate counterparts in the three bandpasses $W1$ [$3.4 \mu\text{m}$], $W2$ [$4.6 \mu\text{m}$] and $W3$ [$12 \mu\text{m}$], while in the lowest frequency band $W4$ [$22 \mu\text{m}$] photometric data is available only for five of these sources. The remaining 6 sources were detected only in the $W1$ and $W2$ bands and therefore only one colour is available. Note also that the uncertainty of the $W3$ magnitude of SDSS J174402.91+463740.7 is not given in the VIZIER database, and therefore the reported magnitude should be considered as an upper limit. We computed the $W1 - W2$ and $W2 - W3$ colours without reddening correction, since all the considered sources have a Galactic latitude higher than 20° . In any case, its largest effect on the colours is of only a few hundredths of magnitude, quite lower than typical uncertainties. The resulting two WISE colour plot that is shown in Figure 1. In this plane γ -ray blazars are essentially concentrated within the two coloured areas, defined in the figures reported in Massaro et al. (2013), D’Abrusco et al. (2014), and Massaro and D’Abrusco (2016): BL Lac objects are mainly concentrated in the blue area, while FSRQ are mostly found in the red one. In their data there is no definite boundary between BL Lac and FSRQ regions, and the given separation is only indicative. All our candidates have colours matching very well the BL Lac region. Note, in particular, the very close similarity between our plot and the one given in Figure 2 of Massaro et al. (2013).

Recently, two new catalogues of blazar candidates has been published (D’Abrusco et al. 2019) based on *WISE* infrared data. WIBRaLS2 contains sources with 4-band photometric data, spatially matched to radio-loud sources, while KDEBLACS collects radio-loud sources with 3-band *WISE* data only, with mid-infrared colors similar to γ -ray confirmed BL Lacs. Association of some of the clusters on our selected samples to those two catalogues are discussed in the following Section.

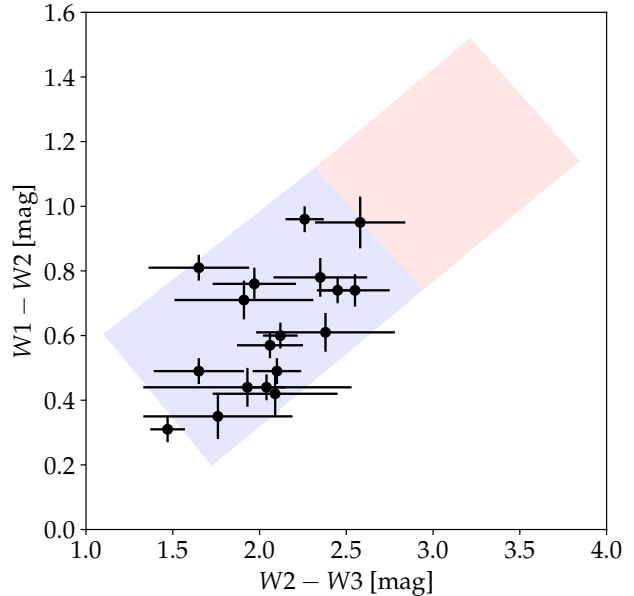


Fig. 1 Plot of the infrared colours of 18 new candidate blazars with data from the AllWISE catalogue. The shaded regions define the WISE Blazar locus (Massaro and D’Abrusco 2016) in which γ -ray loud blazars are present. The blue-shaded region represents the locus where there is a concentration of BL Lac objects, while the red-shaded region correspond to FSRQ objects.

4 Properties of counterparts to individual clusters

4.1 9Y-MST J0013–3222

There are three NVSS radio sources, two of them are also in SUMSS21, within $6'$. The brightest, at the closest angular distance to the γ -ray position equal to $2'71$, is NVSS J001339–322445. It is associated with the X-ray counterpart 1RXS J001338.8–322442.

The ESO DSS⁴ R -band image (Figure 2) is rather peculiar, showing two knots, or galactic nuclei, about $12''$ apart, of similar brightness embedded in an elongated nebular structure. A fainter weaker knot is in the middle the main two. The nebular structure has an extended straight feature, aligned in the same direction of the line connecting the knots, resembling a faint jet.

2dF⁵ spectra of both knots are available: the spectrum of quality $Q = 4$ is typical of an elliptical galaxy without emission lines and a rather low Ca H+K break ratio; the reported redshift is $z = 0.2598$. The radio spectrum is clearly steep at low frequencies: the spectral index from SUMSS21 (0.843 GHz) and NVSS (1.4

⁴<http://archive.eso.org/dss/dss>

⁵<http://www.2dfgrs.net>

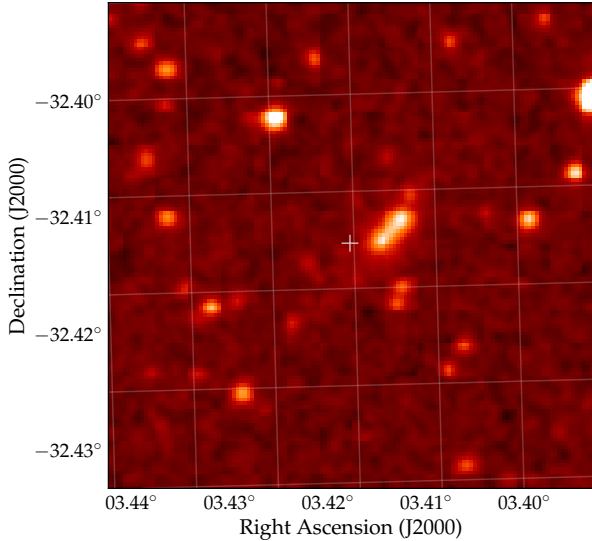


Fig. 2 ESO DSS *R*-band image of the field surrounding NVSS J001339–322445 (white cross).

GHz) is equal to -1.2 , rather close to the value of -1.0 reported at frequencies between 72 and 231 MHz in the GLEAM EGC catalogue (Hurley-Walker et al. 2017) However, there is an indication of a flattening at high frequencies since between 1.4 and 4.85 GHz the spectral index is -0.34 .

This source is also present in the ROXA sample (Turiziani et al. 2007) and its classification is uncertain Radio Galaxy or BL Lac object.

4.2 9Y-MST J0024+2401

This cluster has a well established correspondence at a distance of $0'.8$ with the γ -ray source 4FGL J0024.1+2402, for which no possible counterpart is reported.

There are a few nearby NVSS sources, but the closest and brightest is at $2'.97$ and has the interesting optical counterpart SDSS J002406.10+240438.3: its spectrum (Figure 3) has some features detected by the automatic SDSS procedure with an estimated $z = 0.151$, however with small significance (low $\Delta\chi^2$). It appears as a featureless flat continuum with a blue excess with respect to the typical spectrum of an elliptical galaxy. Furthermore, it corresponds to the mid-IR source AllWISE J002406.10+240438.6, having the colours $W1 - W2 = 0.87$ and $W2 - W3 = 2.22$, close to the centre of the *WISE* Gamma-ray Strip (Massaro and D’Abrusco 2016) and it is included in the KDE-BLLACS sample (D’Abrusco et al. 2019).

The association with a new BL Lac object can be considered as a robust result.

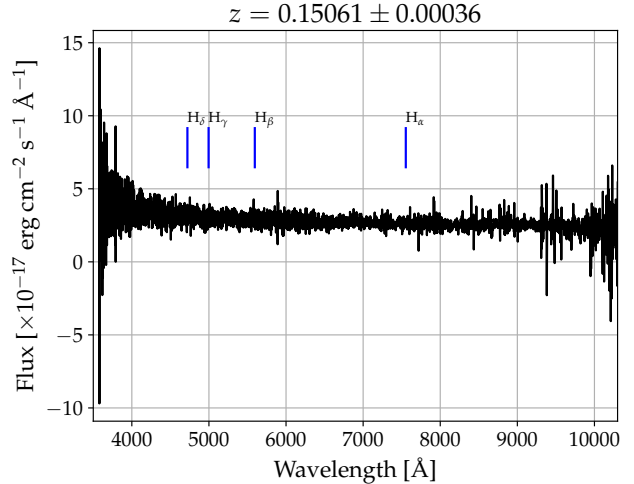


Fig. 3 Sloan Digital Sky Survey optical spectrum (plate no. 7661, fiber no. 398) of SDSS J002406.10+240438.3. Vertical blue segments mark the position of possible Balmer emission lines found by the SDSS automatic analysis.

4.3 9Y-MST J0122+1033

There is only one NVSS source within a distance of $6'$, that has a very likely optical counterpart in SDSS, a starlike source, but unfortunately no spectrum is available. The colour $u - r = 0.63$ is, however, rather blue and well compatible with a quasar. Richards et al. (2015) and Brescia et al. (2015) included this object in their catalogues of candidate quasars, the former also based on the mid-IR *WISE* data (Cutri et al. 2013).

It is therefore a likely blazar candidate, but more information is necessary to confirm the nature of this object.

4.4 9Y-MST J0127+1737

This is a “poor” cluster, having only 4 photons, but with a quite high g that implies a significant M value. There is only one rather faint NVSS radio source within a distance of $6'$. At about $5''$, compatible with the NVSS positional uncertainty, there is a possible faint counterpart in SDSS with $u - r = 0.64$, but no spectrum is available. This source has an interesting mid-IR counterpart in the *WISE* sky with the colours $W1 - W2 = 0.78$ and $W2 - W3 = 2.35$ placing it in the middle of the Gamma-ray blazar strip (Massaro and D’Abrusco 2016) in the BL Lac object section and satisfying the criteria for inclusion in the KDEBLLACS sample (D’Abrusco et al. 2019).

It is reported in the quasar candidate lists by Brescia et al. (2015) and Richards et al. (2015), who give a photometric redshift estimate around 0.5.

It is therefore a good High Energy Peaked BL Lac (HBL) candidate at high redshift which must be confirmed by spectral data.

4.5 9Y-MST J0143–0122

There are several radio sources within a distance of $6'$ and therefore the possibility of a multiple association cannot be excluded. The brightest radio source is NVSS J014317–011858, also reported as PKS J0143–0119 and 4C –01.09. It appears in NVSS but results fragmented in several components of different brightness in FIRST. VLA images (Reid et al. 1999; Roberts et al. 2015) have a core-jet structure with some central bright knots and the peak at extreme west was associated with the optical counterpart by Lacy (2000), a faint object at $z = 0.5194$, confirmed by a SDSS spectrum and exhibiting several broad emission lines (Figure 4). As noticed by Roberts et al. (2015), the nature of this object is still unclear. In particular, it is not established whether it has or not a flat spectrum component embedded in a steep spectrum extended emission. An indication for this possibility is provided by the NRAO VLBA⁶ calibration data and images at 2.3 and 8.6 GHz having only a single compact component with a possibly inverted spectrum. The search in the AllWISE catalogue gives a poorly resolved source J014316.73–011900.6 with mid-IR colours $W1 - W2 = 0.61$ and $W2 - W3 = 2.38$ well located in the BL Lac section of the *WISE* Gamma-ray Strip (Massaro and D’Abrusco 2016).

For the sake of completeness we mention the presence at $6'.6$ of another blazar candidate, the source 2WHSP J014347.1–01260, located just outside the R_{\max} circle, which has an AllWISE counterpart with only the $W1 - W2 = 0.18$ that places it in a marginal position of the WISE strip.

4.6 9Y-MST J0202+2942

This cluster corresponds to 4FGL J0202.4+2943, but no counterpart is given. There is only one NVSS radio source in its environment which has a clear optical starlike counterpart. Unfortunately, no spectrum is available in SDSS but DR15 photometric data give $u - r = 0.86$. It was reported in the quasar samples by Brescia et al. (2015) and Richards et al. (2015). The AllWISE counterpart has the colours $W1 - W2 = 0.73$, $W2 - W3 = 2.44$, $W3 - W4 = 2.04$ which locate it well within the BL Lac segment of the WISE blazar strip used for selecting the WIBRaLS and WIBRaLS2 samples (D’Abrusco et al. 2014; D’Abrusco et al. 2019).

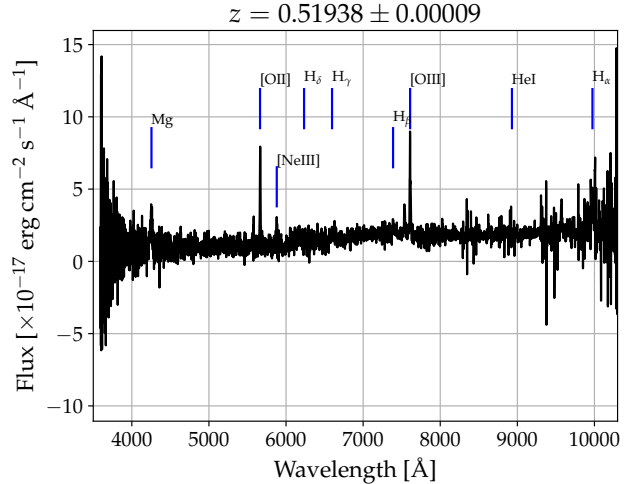


Fig. 4 Sloan Digital Sky Survey optical spectrum (plate no. 4350, fiber no. 783) of the optical counterpart associated to NVSS J014317–011858. Vertical blue lines mark some of the emission features automatically detected in SDSS.

It is therefore likely that this source is a good HBL candidate, whose proper classification requires an optical spectrum.

4.7 9Y-MST J0332+8227

This cluster corresponds to 4FGL J0333.1+8227 and was related to 1RXS J033208.6+822654, classified as ‘bcu’ (i.e. blazar candidate of uncertain type). There is only one NVSS radio source within $6'$ that is at a very close angular distance. The corresponding optical source is very faint and there is no spectral information; however there is a mid-IR counterpart with the colours $W1 - W2 = 0.81$, $W2 - W3 = 1.64$, $W3 - W4 = 3.15$, that place this object in a rather marginal position with respect to the WISE blazar strip, but compatible when the errors are taken into account.

4.8 9Y-MST J0557+7705

This cluster corresponds to the preliminary source FL8Y J0557+7705 but it is not included in the final 4FGL catalogue. There are two NVSS radio sources within $6'$: one is at the close angular distance of $0'.9$, while the other is at $5'.9$, close to R_{\max} but quite higher than R_m . We thus selected the former one as the most likely counterpart. There is no clear source in POSS, but the GAIA DR2⁷ reports an object at about $1''$ having a G_{mag} of 19.2. There is a much brighter counter-

⁶http://www.vlba.nrao.edu/cgi-bin/vlba_calib.cgi

⁷<https://gea.esac.esa.int/archive/>

part in the mid-IR, AllWISE J055721.46+770443.2, detected in three of the four bands and having the colours $W1 - W2 = 0.96$, $W2 - W3 = 2.26$, which locate it close the centre of the *WISE* Gamma-ray Strip in the transition region between BL Lac objects and FSRQ, but it is also included in the KDEBLACS sample (D’Abrusco et al. 2019).

This source was included in the AGN catalogue based on mid-IR data by Secrest et al. (2015).

The available data do not allow a safe classification of the proposed counterpart and more information is necessary to confirm its blazar nature.

4.9 9Y-MST J0650–5146

This cluster corresponds to 4FGL J0650.2–5144, but no counterpart is reported. It lies at a low Galactic latitude in a rather crowded field. There are two SUMSS21 radio sources within $6'$: the brighter one is at $1'8$ and the other at $4'5$. The former has a reasonable optical counterpart, while the latter does not correspond to any bright enough source in POSS. No spectral data are available for this source, but it has a well established counterpart in the mid-IR with 3 band photometric data (Figure 5). The resulting colours ($W1 - W2 = 0.61$, $W2 - W3 = 2.11$) place it among the BL Lac segment of the *WISE* Gamma-ray Strip and it is included in the KDEBLACS catalogue.

We notice also that there is a 3FGL source at about $32'$, without a correspondent cluster in the 9Y-MST catalogue, but that is likely associated with the blazar candidate 2WHSPJ064710.0-51354. Moreover, this latter source corresponds to 4FGL J0647.0–5138, different from the one associated with our cluster.

4.10 9Y-MST J0752+7120

Several NVSS sources are in the surroundings of this cluster. Considering that it is the most compact one in the sample with $R_{\max} = 2'9$ and, therefore, if we limit the search radius to this value, the number of radio sources is reduced to 2, of which only one has an interesting optical counterpart. This source has a good positional correspondence with the X-ray source 1RXS J075225.0+712048 classified a quasar by Flesch (2016). The only available WISE colour $W1 - W2 = 0.5$ is compatible with the BL Lac portion of the blazar strip Massaro and D’Abrusco (2016).

It appears an interesting blazar candidate, but more data are necessary for a correct classification.

4.11 9Y-MST J0947+1120

There are four NVSS sources with fluxes ranging from 3 to 48 mJy, and all are within the $R_{\max} = 4'2$ circle. The brightest source is the elliptical galaxy SDSS

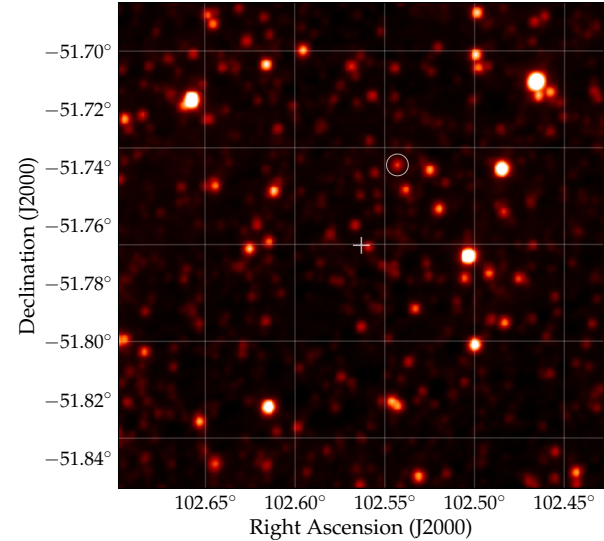


Fig. 5 WISE band 1 ($3.4 \mu\text{m}$) image of the field surrounding 9Y-MST J0650–5146 (whose centroid is marked by the cross). The circle marks its most likely counterpart, as discussed in the main text.

J094745.91+112021.9 at $z = 0.187$, and its spectrum (Figure 6) presents some clear absorption lines; this object was already included in the sample of BL Lac candidates by Plotkin et al. (2008). It is also associated with the X-ray source 2RXS J094746.1+112030. Unfortunately, a close very bright star makes difficult a good mid-IR photometry, thus there is no information on its position in the *WISE* colour plot useful for the blazar classification.

None of the other radio sources has optical counterparts useful for unraveling their nature and thus they are not further considered in the present work.

4.12 9Y-MST J1003–2139

This cluster corresponds to 4FGL J1003.6–2137 which is associated with the ‘bcu’ source 1RXS J100342.0-213752. There is only one NVSS source close to the cluster centroid corresponding to this RASS counterpart, also detected by XMM. The associated optical object is peculiar because of its elongated shape, unresolved in the available images (Figure 7); it is classified as ‘extended’ in the HYPERLEDA database (Makarov et al. 2014). It is possible that it is a very close pair of starlike objects and for this reason its optical magnitude might be brighter than the real value. It has a relatively bright AllWISE counterpart having colours $W1 - W2 = 0.31$, $W2 - W3 = 1.47$, that place this object at the lower end of the *WISE* BL Lac strip.

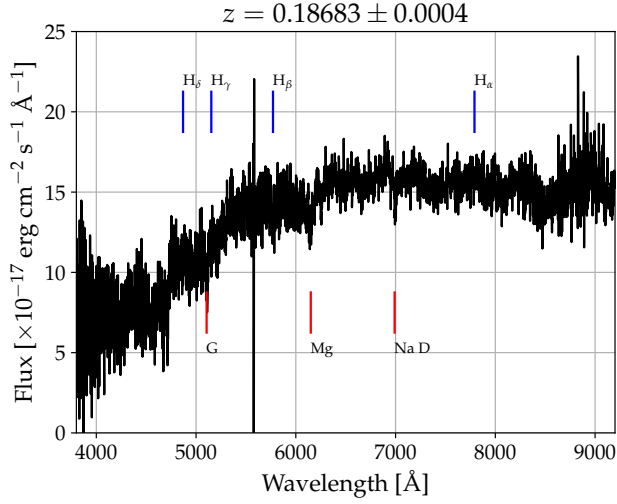


Fig. 6 Sloan Digital Sky Survey optical spectrum (plate no. 1742, fiber no. 37) of SDSS J094745.91+112021.9. Vertical red lines indicate some of the absorption features reported in SDSS. No significant emission line is apparent. Balmer series location is marked by blue vertical lines.

4.13 9Y-MST J1636–0456

This cluster corresponds to 4FGL J1636.5–0454, which is associated to a NVSS source classified as ‘bcu’. There are two NVSS sources close to the cluster centroid, but only one is at an angular distance lower than R_{\max} , the same reported in the 4FGL catalogue, which has also the optical counterpart SDSS J163632.084–045506.0, a galaxy without available spectral data. The $u - r$ colour is equal to 2.41, large for a blazar-like object according to Massaro et al. (2012). It has a mid-IR counterpart whose colours ($W1 - W2 = 0.56$, $W2 - W3 = 2.06$) place it well among BL Lac objects in the *WISE* Gamma-ray Strip and in the KDEBLACS catalogue.

4.14 9Y-MST J1646–0942

This cluster corresponds to 4FGL J1646.0–0942 and the RASS source 1RXS J164602.3–094113 is indicated as counterpart. There are three possible correspondences with NVSS: the closest one, at a separation of $1'29$, is also the most interesting because it can be associated with the above X-ray source. The *WISE* counterpart has only $W1$ and $W2$ photometry, thus it is not possible to verify if it lies within the strip.

4.15 9Y-MST J1714+3227

There are 2 NVSS and 4 FIRST sources in the $6'$ region around this cluster. The source closest to the centroid has very clear optical and mid-IR counterparts:

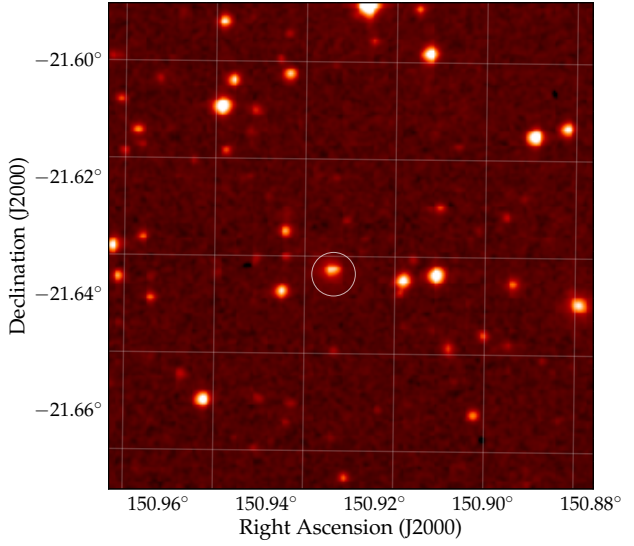


Fig. 7 ESO DSS *R*-band image of the field surrounding 1RXS J100342.0–213752. The peculiar optical counterpart discussed in the text is marked by the white circle.

an elliptical galaxy without a particularly bright and blue nucleus, but with the colours $W1 - W2 = 0.49$, $W2 - W3 = 1.65$ that place it at the lower end of the *WISE* Gamma-ray Strip, and it is included in the KDEBLACS catalogue.

The other and brighter NVSS source does not have an optical counterpart, but there is a *WISE* source with a positional correspondence detected only in the $W1$ and $W2$ bandpasses. The former one is therefore the most likely candidate, but spectral data are required to confirm its blazar nature.

4.16 9Y-MST J1744+4636

Three NVSS sources are within the angular distance of $6'$. However, because it is a compact cluster with $R_{\max} = 3'5$, only the closest source could be a reliable candidate. It has a RASS and XMM counterpart, and the optical one in SDSS is a starlike object with $u - r = 0.80$, but without spectral information. The mid-IR counterpart has peculiar colours: $W1 - W2 = 0.45$, $W2 - W3 = 1.93$ locating it in the BL Lac portion of the *WISE* strip, whereas the very high $W3 - W4 = 3.74$ does not confirm its position in the 3-colour strip. It is in the Brescia et al. (2015) list of candidate quasars. The Spectral Energy Distribution appears dominated by the X-ray emission in the keV band, around 10^{-12} erg cm $^{-2}$ s $^{-1}$, higher than the optical emission by a factor of about 3, typical of extreme HBL objects (Costamante et al. 2001).

4.17 9Y-MST J2024–2234

This is a rather peculiar low- g cluster likely corresponding to 4FGL J2025.3–2231 which has not any reported counterpart. The analysis in a smaller region with $\Lambda_{\text{cut}} = 0.7$ confirms the same structure, while using $\Lambda_{\text{cut}} = 0.5$ a cluster with 8 photons and $g = 2.908$ is found, as reported in Table 1. The position of the latter cluster is much closer to two 4FGL sources and in the $6'$ radius there are two NVSS sources. The faintest and more distant has a weak mid-IR possible counterpart and no more information is available. The closest has a possible optical-mid IR counterpart at about $4''$, moreover it is in the low frequency flat spectrum radio sources LORCAT (Massaro et al. 2014) catalogue. The *WISE* colours $W1 - W2 = 0.76$, $W2 - W3 = 1.98$, $W3 - W4 = 2.68$ locate it in the BL Lac region defined by D'Abrusco et al. (2014). Unfortunately no optical spectrum is available to support this classification.

4.18 9Y-MST J2030–1622

This cluster corresponds to 4FGL J2030.9–1621 for which no counterpart is given. There are three NVSS sources in its environment. The brightest of them, at an angular distance from the centroid of $2'.5$, does not have counterparts either in the optical nor in the mid-IR sky. Therefore, no more indications on its nature can be inferred. The closest source, at a distance of $49''$, has a faint optical counterpart in the POSS corresponding to a mid-IR object with colours $W1 - W2 = 0.71$, $W2 - W3 = 1.91$, locating it in the BL Lac segment of the *WISE* strip and it is included in the KDEBLACS sample.

Finally, also the third and faintest NVSS source is without counterparts in the optical and mid-IR. The second one is therefore currently the most interesting candidate, but spectral data will be useful for confirming its nature.

4.19 9Y-MST 2046–5410

This cluster corresponds to 4FGL J2046.9–5409 source for which no counterpart was reported. There are two SUMSS21 radio sources in its neighborhood at about the same angular distance: the fainter source does not have a clear optical or mid-IR counterpart, while the brighter one (angular distance of $3'.3$) can be associated with a faint optical object also detected in the mid-IR. Its *WISE* colours are $W1 - W2 = 0.42$, $W2 - W3 = 2.09$ which are in the BL Lac section of the *WISE* strip. Close to this position there is a PMN source, that, if associated with our candidate, has a flux density that gives a marginally flat radio spectral index equal to -0.55 .

4.20 9Y-MST J2115–4938

This cluster has the highest g in the sample and corresponds to 4FGL J2115.6–4938. The proposed counterpart is MRSS 235-024179, a galaxy in the Muenster Red Sky Survey including about 5.5 million galaxies with Galactic latitudes less than -45° (Ungruhe et al. 2003). There are two SUMSS21 sources within the search region: one of them is at a distance of $5'.5$, well outside the $R_{\text{max}} \approx 3'$ circle. The closer source, at $1'.1$, has a possible relatively bright optical counterpart well detected in the *WISE* sky with the colours $W1 - W2 = 0.48$, $W2 - W3 = 2.10$ that place it in the BL Lac segment of the strip. Its position agree with that of the above galaxy. Considering the radio flux density reported in PMN, it has a flat spectrum. Therefore, it appears as a reliable blazar candidate.

4.21 9Y-MST J2135–5759

There are three SUMSS21 sources near the centroid position of this object: the closest is at the angular distance of only $0'.4$, and another and brighter object, reported also in the CRATES catalogue, is at $2'.3$. Unfortunately, the latter source does not have a possible optical counterpart, and, taking into account the radio position uncertainty, there is a high source confusion in the *WISE* mid-IR images. Thus, the poor information on this object prevents any reliable identification, although it cannot be excluded as a possible counterpart of the high energy source.

The closer radio source has a possible optical and mid-IR counterpart at an angular distance of about $4''$, that is higher than the SUMSS21 position uncertainty of about $2''$. This object has the mid-IR colours $W1 - W2 = 0.40$, $W2 - W3 = 2.02$ placing it close to end of the BL Lac segment of the *WISE* strip. The third SUMSS21 source, much fainter than the other two, is without possible counterparts. The occurrence of two possible counterparts requires a deeper investigation to disentangle this ambiguity.

4.22 9Y-MST J2240–1244

This cluster corresponds to 4FGL J2240.3–1246, that is associated with the RASS source 1RXS J224014.7-124736. Three NVSS sources are within the $6'$ search radius and all are at distances from the centroid higher than $4'$. Only one has a possible optical counterpart and appears closely associated with the above X-ray source. A local analysis with the much shorter $\Lambda_{\text{cut}} = 0.3\Lambda_m$ gives a more compact cluster closer to this counterpart and marginally satisfying its R_{max} limit. There is a mid-IR counterpart detected only in two bands and

the resulting colour $W1 - W2 = 0.43$ is compatible with a BL Lac object.

4.23 9Y-MST J2240–4747

This cluster corresponds to 4FGL J2240.7–4746 and the reported ‘bcu’ counterpart is the radio source SUMSS J224042–474733. This is only one SUMSS21 source in our search circle. The possible optical counterpart has a distance offset of $3''.8$, higher than the nominal mean positional error of $1''.8$; it has a bright *WISE* counterpart detected in all the four bands. Its mid-IR colours are $W1 - W2 = 0.43$, $W2 - W3 = 2.04$, $W3 - W4 = 2.57$ well compatible with the BL Lac segment of blazar strip.

4.24 9Y-MST J2321–2606

Two NVSS sources are within the search radius: the brighter one is at a distance of $1''.2$ and the other at $4''.9$. The former source has a radio flux density brighter by about a factor of 6 and is included in the HMQ catalogue (Flesch 2015) as a photometric quasar candidate with an estimated z of 0.7. It is well detected in the mid-IR and the *WISE* colours are $W1 - W2 = 0.73$, $W2 - W3 = 2.56$, locating the source near the centre of the WISE strip in the mixed FSRQ and BL Lac objects region, but it is included in the KDEBLACS sample (D’Abrusco et al. 2019).

5 Summary and discussion

The extragalactic γ -ray sky appears dominated by blazar sources (Massaro et al. 2016) and therefore the discovery of new blazars can be driven by the search for counterparts of new high energy sources. In the new γ -ray catalogues there are several sources not yet associated with extragalactic objects. We extracted from the 9Y-MST catalogue a sample of 24 unassociated clusters for which there is at least a radio source at an angular separation from the centroid lower than $6'$. For each of these sources we extended the search to other wavelength ranges to verify if they exhibit some properties allowing a classification as blazar candidates.

Unfortunately, optical spectra were available for only three sources, while two *WISE* colours were obtained for 18 sources, which are located in the BL Lac portion of the blazar strip. We also verified if these possible counterparts are in the most recent catalogues based on mid-IR data and found that only one is in the WIBRaLS2, while other 8 are in the KDEBLACS. In any case, more observations to definitely confirm their nature are needed.

13 of these clusters were also found to be in the recent preliminary version of the 4FGL catalogue (The Fermi-LAT collaboration 2019), confirming the validity of MST findings.

It is interesting that about all objects are BL Lac candidates and the only one with a FSRQ borderline position has a featureless SDSS spectrum. This finding agrees with the results of a previous blazar search (Campana et al. 2016c) in which only three objects in a sample of 30 exhibited mid-IR colours in the FSRQ region. A possible explanation is that our cluster selection at energies higher than 10 GeV is biased to extract BL Lacs, and particularly HBL sources, rather than FSRQs. HBL objects, in fact, have the Compton component in their Spectral Energy Distribution peaking in the GeV range, while for the other blazars it is at lower energies (Abdo et al. 2010; Fan et al. 2016) and therefore faint hard sources are preferentially detected against a softer background. Only the bright radio source PKS J0143–0119 (see Section 4.5), for which an optical spectrum is available, exhibits some emission lines typical of FSRQs but its *WISE* colours are in the BL Lac region, indicating that it could be an outlier. The main aim of the present work is to contribute to the knowledge of the BL Lac population, in particular for what concerns low brightness objects which are easily detected at high energies. Following this approach, a possibility to be explored is to verify the existence of a subclass of BL Lacs too faint in radio band (Massaro et al. 2017) to be marginally detected at the sensitivity level of the available surveys.

We acknowledge use of archival Fermi data. We made large use of the online version of the Roma-BZCAT and of the scientific tools developed at the ASI Space Science Data Center (SSDC), of the final release of 6dFGS archive, of the Sloan Digital Sky Survey (SDSS) archive, of the NED database and other astronomical catalogues distributed in digital form (VizieR and Simbad) at Centre de Données astronomiques de Strasbourg (CDS) at the Louis Pasteur University. This publication makes also use of data products from the Wide-field Infrared Survey Explorer, which is a joint project of the University of California, Los Angeles, and the Jet Propulsion Laboratory/California Institute of Technology, funded by the National Aeronautics and Space Administration.

Compliance with Ethical Standards Conflict of Interest: The authors declare that they have no conflict of interest. Ethical approval: This article does not contain any studies with human participants or animals performed by any of the authors.

Table 1 Coordinates and main properties of the MST clusters detected at energies higher than 10 GeV and of their possible candidate blazar counterparts. Celestial coordinates are J2000, angular distances $\Delta\theta$ are computed between the centroids of MST clusters and those of indicated counterparts. See the main text for discussion.

9Y-MST	RA deg	Dec deg	n	g	M	R_m '	R_{max} '	RA °	Dec °	$\Delta\theta$ '	Counterpart
J0013-3222	3.439	-32.373	10	2.319	23.194	12.7	24.7	3.41413	-32.41265	2.7	ROXA J001339.1-322443.8
J0024+2401	6.028	24.027	8	2.618	20.942	4.98	11.9				
	6.037	24.031	6	3.598	21.587	3.72	5.76	6.02542	24.07731	2.8	SDSS J002406.10+240438.3 ^(a)
J0122+1033	20.617	10.553	4	3.815	15.262	1.14	8.10	20.59842	10.53700	1.5	SDSS J012223.62+103213.2
J0127+1737	21.984	17.627	4	6.428	25.710	1.38	3.30	22.01921	17.60536	2.3	SDSS J012804.61+173619.3
J0143-0122	25.855	-1.373	5	3.541	17.706	2.52	6.30	25.81967	-1.31692	3.8	SDSS J014316.72-011900.9
J0202+2942	30.637	29.709	9	2.953	26.581	7.62	16.0				
	30.633	29.722	4	10.26	41.052	0.42	2.58	30.66542	29.72361	1.8	SDSS J020239.70+294325.0 ^(b)
J0332+8227	53.103	82.451	9	2.761	24.848	4.68	10.7	53.09908	82.44589	0.3	AHWISE J033223.77+822645.1
J0557+7705	89.392	77.087	6	3.883	23.296	3.66	6.78	89.33942	77.07867	0.9	AHWISE J055721.46+770443.2
J0650-5146	102.563	-51.767	11	3.471	38.178	3.54	11.8	102.54304	-51.73942	1.7	AHWISE J065010.33-514421.9
J0752+7120	118.177	71.341	4	5.017	20.069	1.74	2.46	118.10550	71.34722	1.4	AHWISE J075225.32+712050.0
J0947+1120	146.991	11.349	4	4.926	19.702	1.62	4.20	146.94129	11.33942	3.0	SDSS J094745.91+112021.9
J1003-2139	150.894	-21.661	5	5.611	28.057	1.98	5.64	150.92861	-21.63592	2.4	AHWISE J100342.86-213809.3
J1636-0456	249.104	-4.939	7	4.479	31.351	2.88	3.90	249.13367	-4.91833	2.1	SDSS J163632.08-045506.0
J1646-0942	251.500	-9.708	10	3.583	35.831	3.54	7.62	251.50479	-9.68839	1.2	AHWISE J164601.15-094118.2
J1714+3227	258.647	32.450	9	5.249	47.241	2.40	5.76	258.63783	32.46711	1.1	SDSS J171433.08+322801.6
J1744+4636	266.048	46.603	4	4.560	18.239	1.80	3.54	266.01217	46.62797	2.1	SDSS J174402.91+463740.7
J2024-2234	306.219	-22.567	12	2.785	33.424	4.74	13.1				
	306.301	-22.515	8	2.908	23.262	3.48	9.36	306.31321	-22.50511	1.0	AHWISE J202515.17-223018.4 ^(c)
J2030-1622	307.714	-16.377	9	3.014	27.127	2.76	9.18	307.70054	-16.37331	1.1	AHWISE J203048.13-162223.9
J2046-5410	311.686	-54.175	9	4.166	37.496	2.22	8.64	311.75304	-54.21264	3.3	AHWISE J204700.73-541245.5
J2115-4938	318.916	-49.639	5	7.052	35.259	1.86	2.94	318.93613	-49.65195	1.1	AHWISE J211544.67-493907.0
J2135-5759	323.829	-57.999	6	4.057	24.341	2.58	8.64	323.81706	-57.99562	0.4	AHWISE J213516.09-575944.2
J2240-1244	340.122	-12.738	7	3.061	21.428	4.86	9.00	340.06300	-12.79414	4.8	AHWISE J224015.12-124738.9
	340.091	-12.736	4	4.186	16.743	3.06	3.90	340.06300	-12.79414	3.8	AHWISE J224015.12-124738.9 ^(d)
J2240-4747	340.185	-47.785	8	3.858	30.863	1.80	17.3	340.17565	-47.79177	0.6	AHWISE J224042.15-474730.3
J2321-2606	350.445	-26.105	5	4.954	24.769	2.82	6.00	350.44357	-26.08476	1.3	AHWISE J232146.45-260505.1

^(a) Cluster parameters from a local analysis with $\Delta_{cut} = 0.4\Delta_m$; ^(b) Unweighted coordinates and cluster parameters from a local analysis with $\Delta_{cut} = 0.6\Delta_m$; ^(c) Cluster parameters from a local analysis with $\Delta_{cut} = 0.3\Delta_m$; ^(d) Cluster parameters from a local analysis with $\Delta_{cut} = 0.6\Delta_m$.

Table 2 Radio, mid-IR, and optical photometric data of the blazar candidates in Table 1.

Source	F_{rad} mJy	W1 mag	W2 mag	W3 mag	W4 mag	z mag	r mag	u mag
ROXA J001339.1-322443.8	155.7	14.04 0.03	13.85 0.04			16.23		
SDSS J002406.10+240438.3	11.3	15.44 0.05	14.49 0.06	11.91 0.25		19.41	20.05	21.05
SDSS J012223.62+103213.2	13.6	15.15 0.04	14.87 0.08			18.76	19.32	19.95
SDSS J012804.61+173619.3	7.1	15.15 0.04	14.37 0.05	12.02 0.27		20.16	20.77	21.41
SDSS J014316.72-011900.9	848.7	15.01 0.04	14.40 0.05	12.02 0.40		18.88	20.04	21.16
SDSS J020239.70+294325.0	10.1	14.16 0.03	13.42 0.03	10.97 0.12	8.93 0.45	17.84	18.36	19.22
AiWiSE J033223.77+822645.1	6.6	14.62 0.03	13.81 0.03	12.16 0.29	9.02 0.45		19.26F	
AiWiSE J055721.46+770443.2	33.3	14.16 0.03	13.20 0.03	10.94 0.11			19.2 G	
AiWiSE J065010.33-514421.9	38s	13.97 0.02	13.37 0.03	11.25 0.10			17.8 F	
AiWiSE J075225.32+712050.0	8.7	15.17 0.03	14.67 0.05				20.0 G	
SDSS J094745.91+112021.9	48.5					16.89	17.66	19.73
AiWiSE J100342.86-213809.3	11.4	13.39 0.03	13.08 0.03	11.61 0.10			14.76F	
SDSS J163632.08-045506.0	50.7	14.06 0.03	13.49 0.03	11.43 0.19		17.63	18.74	21.15
AiWiSE J164601.15-094118.2	16.4	13.80 0.03	13.35 0.03				18.76F	
SDSS J171433.08+322801.6	17.6	14.19 0.03	13.70 0.03	12.05 0.26		17.17	18.01	20.24
SDSS J174402.91+463740.7	2.8	15.37 0.03	14.93 0.05	13.00 —	9.22 0.49	18.82	19.49	20.29
AiWiSE J202515.17-223018.4	22.3	14.26 0.03	13.50 0.04	11.53 0.24	8.85 0.52		17.94F	
AiWiSE J203048.13-162223.9	14.8	14.76 0.03	14.05 0.05	12.14 0.40			18.7 F	
AiWiSE J204700.73-541245.5	99.5s	14.69 0.03	14.27 0.06	12.18 0.35			19.52F	
AiWiSE J211544.67-493907.0	84.9s	13.77 0.03	13.28 0.03	11.18 0.14			17.74F	
AiWiSE J213516.09-575944.2	65.2s	14.81 0.04	14.46 0.06	12.70 0.43			18.47F	
AiWiSE J224015.12-124738.9	19.7	14.02 0.03	13.59 0.04				16.88F	
AiWiSE J224042.15-474730.3	67.8s	13.34 0.02	12.90 0.03	10.86 0.11	8.29 0.25		16.25F	
AiWiSE J232146.45-260505.1	24.3	14.57 0.03	13.83 0.04	11.28 0.20			19.36F	

s: radio flux density from SUMSS21; r: r mag from SDSS; F: F mag from GSC2.3; G: G mag from STScI.

References

- Abdo, A.A., Ackermann, M., Ajello, M., Allafort, A., Antonini, E., Atwood, W.B., Axelsson, M., Baldini, L., *et al.*: *Astrophys. J.* **715**, 429 (2010)
- Ackermann, M., Ajello, M., Allafort, A., Asano, K., Atwood, W.B., Baldini, L., Ballet, J., Barbiellini, G., *et al.*: *Astrophys. J.* **765**, 54 (2013)
- Ajello, M., Atwood, W.B., Baldini, L., Ballet, J., Barbiellini, G., Bastieri, D., Bellazzini, R., Bissaldi, E., Blandford, R.D., Bloom, E.D., Bonino, R., Bregeon, J., Britto, R.J., Bruel, P., Buehler, R., Buson, S., Cameron, R.A., Caputo, R., Caragiulo, M., Caraveo, P.A., Cavazzuti, E., Cecchi, C., Charles, E., Chekhtman, A., Cheung, C.C., Chiaro, G., Ciprini, S., Cohen, J.M., Costantini, D., Costanza, F., Cuoco, A., Cutini, S., D'Ammando, F., de Palma, F., Desiante, R., Digel, S.W., Di Lalla, N., Di Mauro, M., Di Venere, L., Domínguez, A., Drell, P.S., Dumora, D., Favuzzi, C., Fegan, S.J., Ferrara, E.C., Fortin, P., Franckowiak, A., Fukazawa, Y., Funk, S., Fusco, P., Gargano, F., Gasparrini, D., Giglietto, N., Giommi, P., Giordano, F., Giroletti, M., Glanzman, T., Green, D., Grenier, I.A., Grondin, M.-H., Grove, J.E., Guillemot, L., Guiriec, S., Harding, A.K., Hays, E., Hewitt, J.W., Horan, D., Jóhannesson, G., Kensei, S., Kuss, M., La Mura, G., Larsson, S., Latronico, L., Lemoine-Goumard, M., Li, J., Longo, F., Loparco, F., Lott, B., Lubrano, P., Magill, J.D., Maldera, S., Manfreda, A., Mazziotta, M.N., McEnery, J.E., Meyer, M., Michelson, P.F., Mirabal, N., Mitthumsiri, W., Mizuno, T., Moiseev, A.A., Monzani, M.E., Morselli, A., Moskalenko, I.V., Negro, M., Nuss, E., Ohsugi, T., Omodei, N., Orienti, M., Orlando, E., Palatiello, M., Paliya, V.S., Paneque, D., Perkins, J.S., Persic, M., Pesce-Rollins, M., Piron, F., Porter, T.A., Principe, G., Rainò, S., Rando, R., Razzano, M., Razzaque, S., Reimer, A., Reimer, O., Reposeur, T., Saz Parkinson, P.M., Sgrò, C., Simone, D., Siskind, E.J., Spada, F., Spandre, G., Spinelli, P., Stawarz, L., Suson, D.J., Takahashi, M., Tak, D., Thayer, J.G., Thayer, J.B., Thompson, D.J., Torres, D.F., Torresi, E., Troja, E., Vianello, G., Wood, K., Wood, M.: *Astrophys. J. Suppl. Ser.* **232**, 18 (2017)
- Bernieri, E., Campana, R., Massaro, E., Paggi, A., Tramacere, A.: *Astron. Astrophys.* **551**, 5 (2013)
- Brescia, M., Cavuoti, S., Longo, G.: *Mon. Not. R. Astron. Soc.* **450**, 3893 (2015)
- Campana, R., Massaro, E., Bernieri, E.: *Astrophys. Space Sci.* **361**, 367 (2016a). 1609.06488. doi:10.1007/s10509-016-2947-1
- Campana, R., Massaro, E., Bernieri, E.: *Astrophys. Space Sci.* **361**, 185 (2016b)
- Campana, R., Massaro, E., Bernieri, E.: *Astrophys. Space Sci.* **361**, 183 (2016c)
- Campana, R., Massaro, E., Bernieri, E.: *Astron. Astrophys.* **619**, 23 (2018)
- Campana, R., Massaro, E., Gasparrini, D., Cutini, S., Tramacere, A.: *Mon. Not. R. Astron. Soc.* **383**, 1166 (2008)
- Campana, R., Bernieri, E., Massaro, E., Tinebra, F., Tosti, G.: *Astrophys. Space Sci.* **347**, 169 (2013)
- Campana, R., Massaro, E., Bernieri, E., D'Amato, Q.: *Astrophys. Space Sci.* **360**, 19 (2015)
- Campana, R., Maselli, A., Bernieri, E., Massaro, E.: *Mon. Not. R. Astron. Soc.* **465**, 2784 (2017)
- Costamante, L., Ghisellini, G., Giommi, P., Tagliaferri, G., Celotti, A., Chiaberge, M., Fossati, G., Maraschi, L., Tavecchio, F., Treves, A., Wolter, A.: *Astron. Astrophys.* **371**, 512 (2001)
- Cutri, R.M., Wright, E.L., Conrow, T., Fowler, J.W., Eisenhardt, P.R.M., Grillmair, C., Kirkpatrick, J.D., Masci, F., *et al.*: Explanatory Supplement to the AllWISE Data Release Products. Technical report, (November 2013)
- D'Abrusco, R., Massaro, F., Paggi, A., Smith, H.A., Masetti, N., Landoni, M., Tosti, G.: *Astrophys. J. Suppl. Ser.* **215**, 14 (2014)
- D'Abrusco, R., Álvarez Crespo, N., Massaro, F., Campana, R., Chavushyan, V., Landoni, M., La Franca, F., Masetti, N., Milisavljevic, D., Paggi, A.: *Astrophys. J. Suppl. Ser.* **242**(1), 4 (2019)
- Fan, J.H., Yang, J.H., Liu, Y., Luo, G.Y., Lin, C., Yuan, Y.H., Xiao, H.B., Zhou, A.Y., Hua, T.X., Pei, Z.Y.: *Astrophys. J. Suppl. Ser.* **226**(2), 20 (2016)
- Flesch, E.W.: *Proc. Astron. Soc. Aust.* **32**, 010 (2015)
- Flesch, E.W.: *Proc. Astron. Soc. Aust.* **33**, 052 (2016)
- Hurley-Walker, N., Callingham, J.R., Hancock, P.J., Franzen, T.M.O., Hindson, L., Kapińska, A.D., Morgan, J., Ofringa, A.R., Wayth, R.B., Wu, C., Zheng, Q., Murphy, T., Bell, M.E., Dwarakanath, K.S., For, B., Gaensler, B.M., Johnston-Hollitt, M., Lenc, E., Procopio, P., Staveley-Smith, L., Ekers, R., Bowman, J.D., Briggs, F., Cappallo, R.J., Deshpande, A.A., Greenhill, L., Hazelton, B.J., Kaplan, D.L., Lonsdale, C.J., McWhirter, S.R., Mitchell, D.A., Morales, M.F., Morgan, E., Oberoi, D., Ord, S.M., Prabu, T., Shankar, N.U., Srivani, K.S., Subrahmanyam, R., Tingay, S.J., Webster, R.L., Williams, A., Williams, C.L.: *Mon. Not. R. Astron. Soc.* **464**, 1146 (2017)
- Lacy, M.: *Astrophys. J. Lett.* **536**, 1 (2000)
- Makarov, D., Prugniel, P., Terekhova, N., Courtois, H., Vauglin, I.: *Astron. Astrophys.* **570**, 13 (2014)
- Massaro, E., Nesci, R., Piranomonte, S.: *Mon. Not. R. Astron. Soc.* **422**, 2322 (2012)
- Massaro, E., Maselli, A., Leto, C., *et al.*: Multifrequency Catalogue of Blazars, 5th edn. Aracne Editrice, Rome (2014)
- Massaro, F., D'Abrusco, R.: *Astrophys. J.* **827**, 67 (2016)
- Massaro, F., Thompson, D.J., Ferrara, E.C.: *Astron. Astrophys. Rev.* **24**, 2 (2016)
- Massaro, F., Paggi, A., Errando, M., D'Abrusco, R., Masetti, N., Tosti, G., Funk, S.: *Astrophys. J. Suppl. Ser.* **207**, 16 (2013)
- Massaro, F., Marchesini, E.J., D'Abrusco, R., Masetti, N., Andruchow, I., Smith, H.A.: *Astrophys. J.* **834**, 113 (2017)
- Mattox, J.R., Bertsch, D.L., Chiang, J., Dingus, B.L., Digel, S.W., Esposito, J.A., Fierro, J.M., Hartman, R.C., Hunter, S.D., Kanbach, G., Kniffen, D.A., Lin, Y.C., Macomb, D.J., Mayer-Hasselwander, H.A., Michelson, P.F., von Montigny, C., Mukherjee, R., Nolan, P.L., Ramanamurthy, P.V., Schneid, E., Sreekumar, P., Thompson, D.J., Willis, T.D.: *Astrophys. J.* **461**, 396 (1996). doi:10.1086/177068

- Plotkin, R.M., Anderson, S.F., Hall, P.B., Margon, B., Voges, W., Schneider, D.P., Stinson, G., York, D.G.: *Astron. J.* **135**, 2453 (2008)
- Reid, R.I., Kronberg, P.P., Perley, R.A.: *Astrophys. J. Suppl. Ser.* **124**, 285 (1999)
- Richards, G.T., Myers, A.D., Peters, C.M., Krawczyk, C.M., Chase, G., Ross, N.P., Fan, X., Jiang, L., Lacy, M., McGreer, I.D., Trump, J.R., Riegel, R.N.: *Astrophys. J. Suppl. Ser.* **219**, 39 (2015). 1507.07788
- Roberts, D.H., Cohen, J.P., Lu, J., Saripalli, L., Subrahmanyam, R.: *Astrophys. J. Suppl. Ser.* **220**, 7 (2015)
- Secrest, N.J., Dudik, R.P., Dorland, B.N., Zacharias, N., Makarov, V., Fey, A., Frouard, J., Finch, C.: *Astrophys. J. Suppl. Ser.* **221**, 12 (2015)
- The Fermi-LAT collaboration: arXiv e-prints (2019). 1902.10045
- Turriziani, S., Cavazzuti, E., Giommi, P.: *Astron. Astrophys.* **472**, 699 (2007)
- Ungerhe, R., Seitter, W.C., Duerbeck, H.W.: *Journal of Astronomical Data* **9** (2003)